PROPERTIES OF A COLLOIDAL ALUMINA-BONDED TiB_2 COATING ON CATHODE CARBON MATERIALS

H.A. Øye
Institute of Inorganic Chemistry, The Norwegian University of Science and Technology, 7034 Trondheim, Norway

V. de Nora, J.-J. Duruz, G. Johnston
MOLTECH S.A., 9 Route de Troinex, 1227 Carouge, Geneva, Switzerland

ABSTRACT

Laboratory studies of colloidal alumina-bonded TiB_2 have been carried out. The following properties have been demonstrated: The thermal expansion was somewhat higher than for carbon materials, the electrical conductivity was of the same order as graphite, while porosity of the coating was ≈ 30 %. The coating protected by infiltrated aluminium exhibited a high resistance to sodium attack. The material had a strong adherence to carbon materials even after thermal cycling. Other properties include high abrasion resistance of the coating and wettability by liquid aluminium. The coating is an effective barrier to sodium penetration. The barrier action is due to the ability to form a stable liquid aluminium layer in the pores of the coating. Then aluminium, electrolyte and the sodium stabilizing carbon are no longer in close contact and sodium penetration is limited by slow diffusion through the aluminium layer.

INTRODUCTION

Colloidal alumina-bonded TiB_2*) [1, 2] has until now been applied as a coating on different qualities of carbon cathodes for aluminium production in several smelters. Some results from the industrial testing have already been reported [3-5]. It was demonstrated that such an alumina-bonded TiB_2 coating reduces the rate of sodium penetration. The resulting sodium concentration gradient in the start-up phase becomes very small with an expected reduction of mechanical stresses [5]. The present paper gives results from some laboratory studies in order to facilitate a better understanding of the properties of this coating and how it affects the process of aluminium electrowinning in Hall-Heroult cells.

The TiB_2 coating is made from a slurry of fine TiB_2 powder and colloidal alumina. The slurry is applied to cathode blocks in assembled cells in successive layers until a thickness of approximately 1 mm is obtained. The alumina-bonded TiB_2 layer is calcined *in situ* during the cell start-up procedure by resistance heating with a coke layer or by gas or oil burners. An aluminium sheet is used to protect the layer against mechanical damage and oxidation.

Properties of Bulk Alumina-bonded TiB_2

Bulk samples of alumina-bonded TiB_2 were made by slip-casting plaques with thickness up to 10 mm. The samples were subsequently calcined to 1000°C, for 10 hours in a coke bed. This procedure gives a more porous structure than when applied as a coating. A prismatic sample 19.4 x 8.9 x 61.5 mm of 2.36 g/cm^3 density which corresponds to a porosity of 48 % was made. The thermal expansion was determined and compared with some typical commercial carbon cathode materials (Fig. 1). The alumina-bonded TiB_2 material expands 0.56 %, between room temperature and 950°C compared to 0.3 - 0.4 % for the carbon materials, the difference being smallest to some of the semigraphitized materials (~ 0.16 %).

The electrical resistivity of the same sample was determined to be 10.2 μΩm at room temperature. This value is of the same order as graphitized materials, see p. 162 in ref. [6]. At operating temperatures the effective electrical resistivity should become lower as the pores are filled with liquid aluminium which has a resistivity at 950°C of 0.285 μΩm [7].

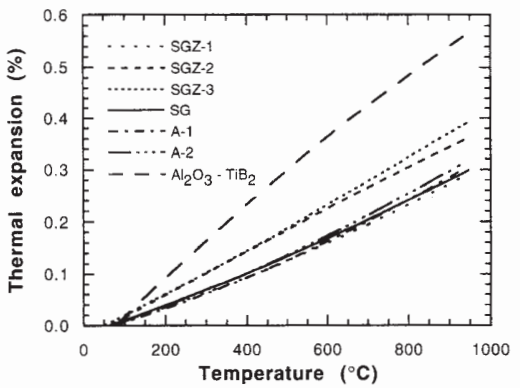

Figure 1: Thermal expansion of bulk alumina-bonded TiB_2 compared with some commercial cathode materials. SGZ: Semigraphitized, SG: Semigraphitic, A: Anthracitic material with some graphite mixed in.

Resistance to Sodium

Sodium enters the carbon cathode surface by the interfacial reaction

$$\text{Al (l)} + 3\ \text{NaF (electrolyte)} = 3\ \text{Na (in C cathode)} + \text{AlF}_3\ \text{(electrolyte)} \qquad (1)$$

and it is desirable to reduce or suppress the absorption of sodium into carbon as it can lead to cathode degradation in aluminium cells. Since it is known that graphitic materials have greater resistance to attack by sodium vapour as compared to amorphous materials (ref. [6] p. 274) it was decided to determine to what extent the alumina-bonded TiB_2 resists or modifies the sodium penetration.

*) Registered trade name: TINOR

A. Tomsett and J. Johnson (Eds.), *Essential Readings in Light Metals*

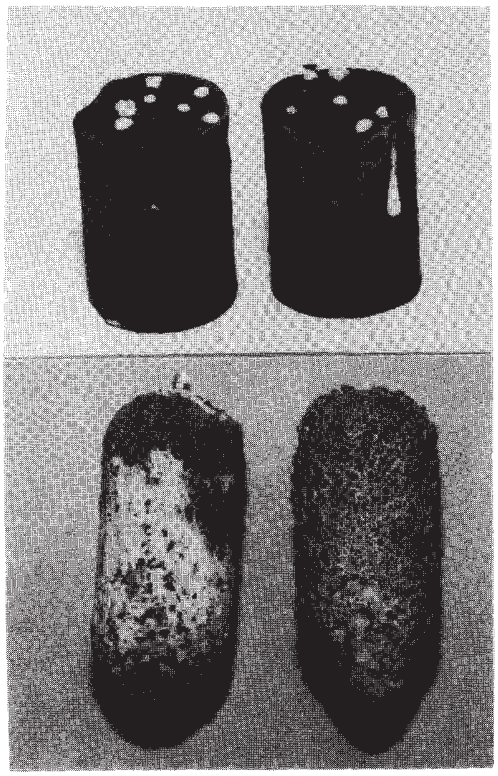

Figure 2: Alumina-bonded TiB_2 samples after the sodium vapour test. a) Bulk samples B1 and B2. b) Coated and electrolysed samples SG3, SG4.

The resistance against sodium attack was tested for 14 mm Ø x 19 mm bulk alumina-bonded TiB_2 samples (Table I). The same equipment and procedures as described for carbon were used (pages 243-44 in reference [6]). As shown in Table I and Fig. 2a the bulk samples were not adversely affected by sodium vapour despite the amount of sodium absorbed being in the range 14 - 19 % as compared to carbonaceous materials which absorb typically 5 to 8 % [8].

Carbon samples with a coating of the colloidal alumina-bonded TiB_2 were tested in the same manner. The sample dimensions were Ø 15 x 30 mm while the edges were rounded. Coated samples that had been heat-treated at 950°C did not give good sodium resistance as the coating peeled off during the test. The samples were then first electrolysed for 1.5 or 2 h in a cryolitic bath with cryolite ratio = 2.4 (CR = mole NaF / mole AlF_3) at 1000°C and current density 1.0 A/cm^2 so that aluminium (as well as some sodium) penetrated into the pores of the alumina-bonded TiB_2 coating before testing. For these specimens no attack could be seen after electrolysis and neither the heat-treated nor the as-prepared samples were attacked by the subsequent sodium vapour test (Table I and Fig. 2b). Hence it can be concluded that the liquid aluminium protects the alumina-bonded TiB_2 coating and consequently the coated carbon cathode, although sodium can be absorbed by the carbon before the coating is infiltrated with aluminium.

Properties of the Alumina-Bonded TiB_2 Coating after Preheating

Laboratory experiments were carried out in order to simulate the conditions when a coated cathode is preheated electrically in a commercial cell. The main object of the tests was to evaluate the baked coating for cracking or delamination and any influence of the thin aluminium sheet placed between the alumina-bonded TiB_2 coated cathode surface and the resistor coke layer. A similar evaluation was performed for the coating applied to ramming paste. A hole (Ø 42 x 45 mm) was then drilled in the centre of the cathode block and manually rammed with cold ramming paste until the surface of the rammed area was flush with the surface of the cathode block. A total of 100 g ramming paste was utilized. The entire surface of the cathode block was then coated with the alumina-bonded TiB_2 to a thickness of about 1 mm.

The experimental set-up is shown in Fig. 3. Commercially available graphite (ELLOR 18) was utilized to prepare anode samples of dimensions Ø 102 x 115 mm height. Commercial anthracitic cathode blocks (70 % anthracite, 30 % graphite) were used for the cathode samples with dimensions Ø 145 x 60 mm. The anode was deliberately made smaller than the cathode to simulate the temperature gradients occurring on the cathode surface between the anode blocks during actual cell preheat. The aluminium sheet was 0.04 to 1 mm thick and the resistor coke layer was 30 mm thick.

Table I Results of Sodium Vapour Resistance Tests of Alumina-Bonded TiB_2

Bulk samples				Samples with coating			
Sample designation	Weight before (g)	Weight increase (%)	Visual evaluation*)	Sample designation	Coating thickness (mm)	Heat treatment 950°C for 10 h before electrolysis	Visual evaluation*)
B 1	9.50	13.8	+	A 1	0.2	Yes	+
B 2	9.16	15.1	(-)	A 2	0.3	Yes	+
B 3	8.77	14.3	+	A 3	0.2	No	+
B 4	9.00	14.4	+	A 4	0.3	No	+
B 5	8.94	19.4	(-)	SG 1	0.2	Yes	+
B 6	8.17	16.1	(-)	SG 2	0.1	Yes	+
B 7	9.79	15.0	(-)	SG 3	0.2	No	+
B 8	8.76	15.0	(-)	SG 4	0.3	No	+

B: Bulk alumina-bonded TiB_2. A: Electrocalcined anthracite with 30% graphite as filler, baked to about 1200°C. SG: Graphite as a filler, baked to about 1200°C. All the samples had small amounts of Na in the form of dots on the surface.
*) – – –: Extreme cracking, —: Heavy to moderate cracking, –: Hairline cracks, little damage,
(-): Thin flakes peeled off. +: No effect.

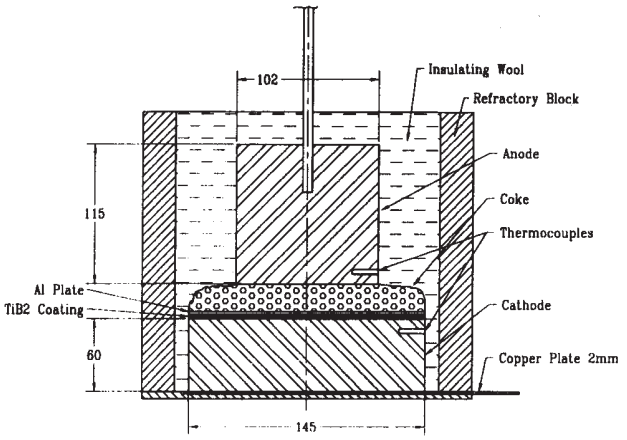

Figure 3: Experimental set-up for simulation of electrical heat-up of cathodes with an alumina-bonded TiB_2 coating.

Thermocouples were placed near the surface of the cathode block and at the bottom of the anode. The cell current and voltage were continuously monitored during the experiment. A weight was placed upon the anode which exerted a pressure of 100 g/cm^2 on the cathode surface comparable to that of real anodes in commercial cells. Table II gives the specifications of the TiB_2 layer and the test conditions.

Table II Experimental Conditions for Preheat Experiments

Sample No.	Coating thickness mm	TiB_2 loading kg/m^2	Thickness of aluminium sheet (mm)	Cathode current density (A/cm^2)	Heating cycle
1	1.0	3.14	-	1.30	14h RT → 800°C 800°C for 1h
2	1.0	3.14	0.04	0.65 for 4h 0.90 for 5h 1.00 for 2h	10h RT → 880°C 880°C for 1h
3	0.8	2.34	-	1.00	7h RT → 880°C 880°C for 1h
4	0.8	2.28	1.0	1.00	9h RT → 780°C 780°C for 3h
5	0.8	2.50	2.0	0.90→1.43	9h RT → 735°C 735°C for 1h
6*	0.8	2.07	2.0	0.3 → 1.21	26h RT → 855°C 855°C for 5h

* The cathode block was rammed with cold ramming paste as described in text.

Heat-up of the coating without the aluminium sheet or foil (Sample 3) gave a characteristic yellow/brown colour associated with the oxidation to TiO_2 and B_2O_3 on the surface (Fig. 4a). A slight oxidation was observed using the thin foil (Sample 2) but the aluminium sheet (Samples 4 and 5) effectively protected the TiB_2 coating against oxidation (Fig. 4c). The absence of oxidation was confirmed by microprobe analysis using electron microscope. The aluminium sheets (1 and 2 mm) acted also as a mechanical protection. This is important in the low temperature region before the coating has been calcined and reached its final hardness. At the end of calcination, the aluminium sheet melted but did not penetrate into the coating. After cooling, the aluminium separated easily from

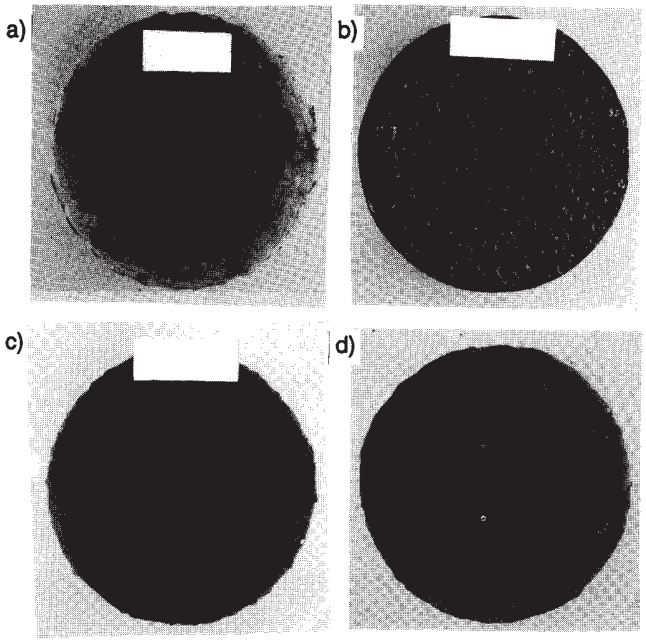

Figure 4: Cathodes after heat treatment. a) Sample 3 without aluminium sheet. b) Sample 4 with the aluminium sheet. c) Sample 4 with the aluminium sheet removed. d) Sample 6 with ramming paste at the centre. (The small holes were due to sampling.)

the coating and an imprint of the coke layer could be seen on its upper surface (Fig. 4b). Figure 4a-d demonstrates that the heat-up did not cause delamination or significant cracking of the TiB_2 coating above the cathode samples or the unbaked ramming paste. The preheating experiments also showed that liquid aluminium does not wet TiB_2 just by heating up to the operating temperature. Dipping carbon samples with TiB_2 coating into liquid aluminium with or without current did not accomplish wetting either.

The cold specimens that had undergone the preheating cycle conditions, similar to that of commercial cells, displayed some hairline cracks perpendicular to the cathode surface (Fig. 5a, b). These were characteristic of cooling cracks and they are not expected to occur when the cathode is maintained at operating temperature. The coating adhered well to the porous structure of the carbon (Fig. 5). Figure 6 shows a secondary electron (SE) image of sample 4. The highly porous structure is seen. Several other BSE and SE pictures as well as element mapping analyses were taken at different locations in the coating. No discernible differences in the grain structures were observed which indicates that the structure is uniform. As expected titanium and boron are found to be the predominant elements. In some grains the aluminium and oxygen content is particularly high which may be the result of a surface coverage of the TiB_2 grains by the colloidal alumina. Variable current density and top temperature did not appear to influence the coating structure. Figure 7 shows an electron mapping of the coating for a sample that has been electrolysed. Wetting is accomplished, and the very porous structure is filled with metallic aluminium.

Adhesion Strength between the Alumina-Bonded TiB_2 Coating and Cathode Carbon Materials

Although the SEM pictures (Fig. 5) already demonstrated that the TiB_2 coating was well anchored to the carbon surface, quantitative

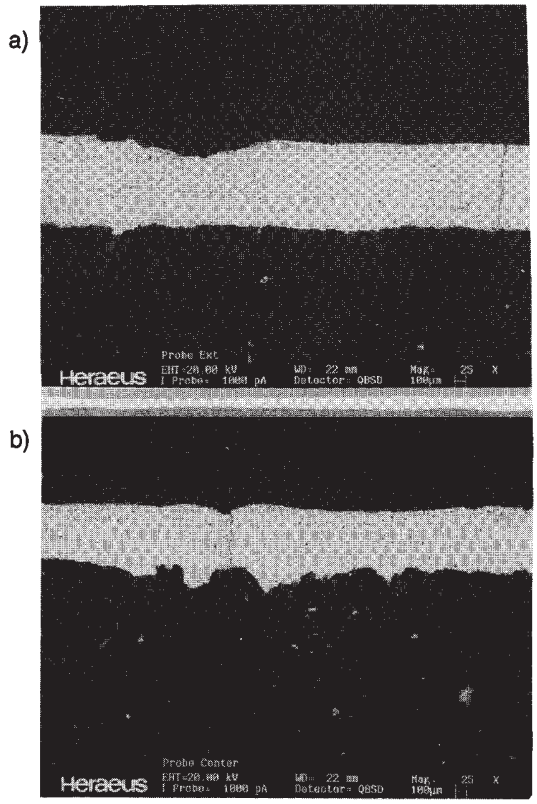

Figure 5: Back scattering, (BS) image of cathode sample 5 after heat treatment and removal of the aluminium sheet. a) At the outer part of the cathode. b) in the centre point of the cathode.

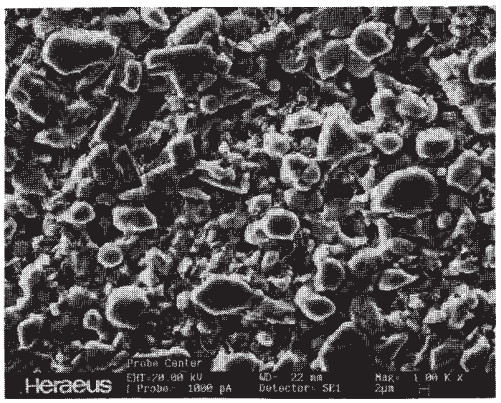

Figure 6: Secondary electron scattering image of sample 5 after heat-treatment. The picture is taken in the centre of the coating.

data on the strength of the adhesion were also desired. Two types of cylindrical cathode material samples (anthracite with 30 % graphite and a semigraphitic material) were coated with the alumina-bonded TiB_2, either 1 brushed layer and 3 layers applied by dipping or 2 brushed layers. The coated materials were dried in air. The diameter of the cylinder before coating was measured, and the thickness of the samples was measured after coating, allowing the coating thickness to be determined (1.7 and 0.3 mm, respectively).

The adhesion-strength was determined by a method developed by Sørgård and Øye [9]. The alumina-TiB_2 coated cylinders were placed in a steel cylinder with a steel ring at the bottom to centre the samples (Fig. 8a). Standard ramming paste was filled into the cylinder and a steel ring (S) was placed on the top. The cylinder with the paste and cathode material was heated up to 40°C before ramming. The paste was then rammed (100 times) to a height of 35 mm and a density of 1.58 g/cm^3, with a standard Sand Rammer Type PRA (Georg Fischer Ltd., Schaffhausen, Switzerland) to give a density of approximately 94 % theoretical. The steel cylinder and rings were then removed. Before baking the ramming paste was surrounded by two half rings of stainless steel, precisely adjusted to the circumference of the paste. Finally the stainless steel ring was surrounded by a strong graphite ring, shown in Fig. 8 b. The samples were placed in a stainless steel container (SIS 2361), and covered by a layer of coke. The samples were then heated at 50°C/h and kept at 990°C for 4 hours. A calculation shows that this set-up would give a net pressure as the unpressurized radial dimension would diminish by 0.05 %.

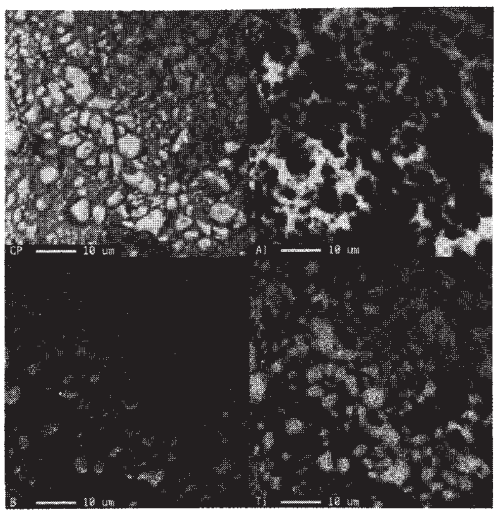

Figure 7: Electron mapping of a TiB_2-coating after electrolysis.

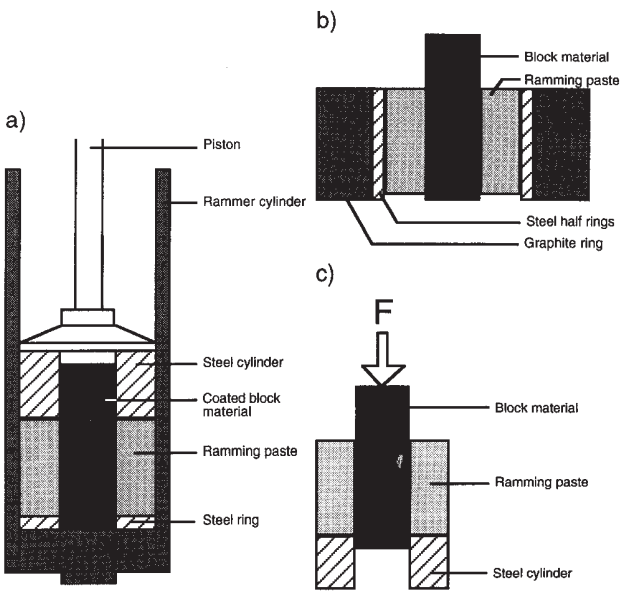

Figure 8: Experimental set-up for determination of adhesion at room temperature. a) Ramming of the sample. b) Baking. c) Determination of adhesion.

The cathode sample was pressed out of the paste at room temperature by use of a Lloyd Universal Testing Machine (Lloyd Instruments Ltd., England) (0-100 kN) with an accuracy of 0.5 % (Fig. 8 c). The maximum load for each sample was registered by a computer. The adhesion-strength was calculated from the following equation:

$$K = \frac{P}{\Pi dh} \qquad (2)$$

where K is the adhesion-strength in MPa
P is the pressing force in N
d is the diameter of the cathode sample in m
h is the height of the ramming paste in m.

The adhesion strength is given in Table III.

Table III The Adhesion-Strength before Breaking for the Alumina-Bonded TiB_2 Coated Carbon Samples

	Adhesion-strength, MPa		
	# 1	# 2	Ave.
Anthracite + 4 layers TiB_2	2.37	2.37	2.37
Anthracite + 2 layers TiB_2	3.43	2.90	3.18
Semigraphite + 4 layers TiB_2	2.65	1.92	2.29
Semigraphite + 2 layers TiB_2	3.63	2.74	3.23
Semigraphite + 2 layers TiB_2*)	3.91	2.65	3.23

*) Sample turned upside down.

In most cases the ramming paste was the weakest material with cracks often apparent in the baked paste. For the semigraphitic sample with 2 layers of alumina-bonded TiB_2 coating the cathode sample itself broke. The samples were then turned upside down and measured again resulting in a crack in the ramming paste. In no instances did the coating delaminate. Therefore the values given in Table III most likely are a measure of the mechanical strength of the ramming paste. The deviations between the two samples are rather large but it should be noted that the values are all considerably higher than for similar experiments with uncoated carbon samples [9]. The adhesion pressures on these samples were never above 1 MPa and usually between 0.4 and 0.8 MPa. As the breakage was in the ramming paste or in the cathode block, the experiments hence show excellent adhesion of the alumina-bonded TiB_2 coating both to the cathode material and to the ramming paste even after cooling down to room temperature.

Stability of the Coating versus Abrasion and Dissolution

Considerations in the choice of cathode blocks include:

1. High electrical conductivity.
2. Low sodium expansion.
3. High thermal shock resistance.
4. High abrasive resistance.
5. Low price.

The trend in the industry is to use more graphitic materials which have advantages with respect to the first 3 points. Graphitic materials are, however, softer than anthracitic materials and are expected to have a lower abrasive resistance.

Cathode wear is caused by physical abrasion due to the movement of Al_2O_3 particles and chemical wear due to the formation of Al_4C_3, especially at the liquid metal-melt interface [6]. Recent experiments indicate that the chemical wear near the aluminium-melt interface is much stronger than any abrasive action due to the movement of Al_2O_3 particles [10]. It is also found that the chemical wear is not very dependent on the graphitization of the carbon material [11]. These two observations combined with the practical experience in commercial cells that graphitic carbon cathode wear is faster than anthracitic, point to physical abrasion as an important wear mechanism for graphitic blocks. This wear becomes of great importance with the increased use of the abrasion prone graphitic materials when at the same time increased cell life is wanted.

A method for the determination of pure physical abrasion has recently been developed [12]. The samples were rotated in a slurry of alumina, dispersed in an aqueous sodium polytungstate solution (Fig. 9). The high density of the liquid (2.60 g/cm^3) kept the alumina evenly dispersed even at velocities as low as 0.4 m/sec. This velocity is comparable to velocities measured in production cells [13], but the velocities may be higher near the tapping spout. The abrasion of test samples was measured against a graphite reference sample. The velocity was about 1.5 m/sec in the comparative experiments in order to get a reasonable abrasion in 4 - 10 hours. A thorough study of the wear as a function of velocity, viscosity and slurry concentration established that frictional wear was the major wear mechanism for velocities up to 2 m/sec [12].

Some of the results of this work are given in Table IV. It should be noted that the wear of semigraphitized, semigraphitic and anthracitic materials relative to graphite is in the same order as experienced in practice.

A semigraphitized material was then coated with alumina-bonded TiB_2 and heat-treated under a bed of resistor coke (heating rate 1°C/min for 16 hours, maintained at 950°C for 10 hours and cooled down naturally to room temperature) before being tested for abrasion resistance. The results for the coated materials are also given in Table IV and compared with the abrasion resistance of commercial uncoated carbon materials. The alumina-bonded TiB_2 coated material has the highest abrasion resistance in spite of the fact that it is applied to a very abrasion prone semigraphitized (SGZ) material. In addition Al_4C_3 formation will not be a corrosion mechanism as no carbon is present in the coating. Therefore, it can be concluded that the major wear mechanism for the alumina-bonded TiB_2 coating will not be abrasion but slow dissolution in liquid aluminium.

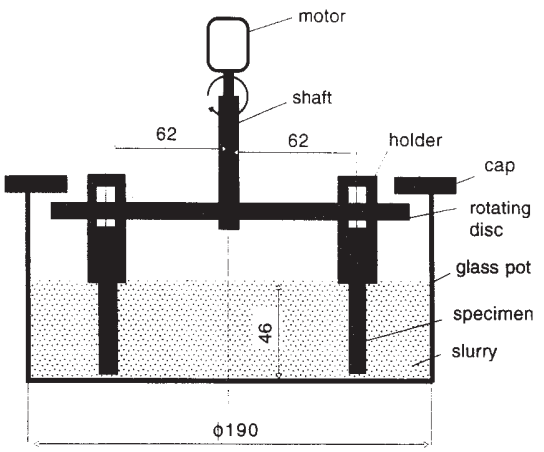

Figure 9: Set-up for room temperature abrasion tests, dimensions in mm.

Table IV Ranking of Abrasive Wear of Carbon Cathode Materials Relative to CS Graphite (Union Carbide) = 100, Alumina Concentration: 1.30 – 1.34 g/ml, Velocity: 1.46 – 1.65 m/s, Time: 4 – 10 hrs [12].

	Cathode material	Relative wear rate*)					Standard deviation
		1	2	3	4	Ave.	
1	SGZ C coated with alumina-bonded TiB_2	5.7 (0.27)***	11.2 (0.35)	7.0 (0.27)	12.4 (0.22)	**9.1**	3.2
2	An. C**	10.2	12.5	9.6	13.4	**11.4**	1.8
3	An. B**	17.1	16.7	20.6	15.2	**17.4**	2.3
4	An. A	16.5	14.5	18.3	21.8	**17.8**	3.1
5	SG A	64.3	72.5	66.4	68.8	**68.0**	3.5
6	SG B	82.3	76.5	79.5	71.2	**77.4**	4.7
7	SGZ A	88.6	84.1	86.5	90.3	**87.4**	2.7
8	G (CS)	101.2	97.6	97.0	102.7	**99.6**	2.8
9	SGZ C	99.4	103.9	97.7	106.8	**102.0**	4.2
10	SGZ B	127.8	131.1	136.8	135.2	**132.7**	4.1

G Graphite: Union Carbide (CS grade).
SGZ Semigraphitized carbon: The whole block (filler and binder) consisting of graphitizable materials has been treated to about 2300-2700°C.
SG Semigraphitic carbon. The aggregate is graphitized but the block (binder coke) has only been heated to normal baking temperatures (≈1200°C).
An. Anthracitic carbon: None or only part of the filler material is graphitized. The block is baked to ≈1200°C. Filler material, usually electrocalcined anthracite, and due to the process some of the material is graphitized. Graphitic filler material is added to the material. The addition is usually in the range of 20 - 60 wt% of the dry aggregate.
Ave. Average.
* Typical wear rate at velocity 1.55 m/s and alumina concentration 1.32 g/ml is 32 mm^3/h.
** Sidewall materials.
*** Layer thickness in mm.

The dissolution of the alumina-bonded TiB_2 coating has been studied under industrial conditions in 150 kA prebake cells [14, 5]. The concentrations of Ti and B in aluminium were analysed in coated and uncoated reference cells (Fig. 10). Average values from 50 to 130 days are:

Cell with coating of alumina-bonded TiB_2: 41.3 ppm Ti, 16.5 ppm B.
Uncoated reference cells: 11.0 ppm Ti, 2.7 ppm B.

Assuming the metal in the coated cells is saturated with TiB_2 these concentrations give a solubility product of $(41.3)\cdot(16.5)^2 = 1.12\cdot10^4$

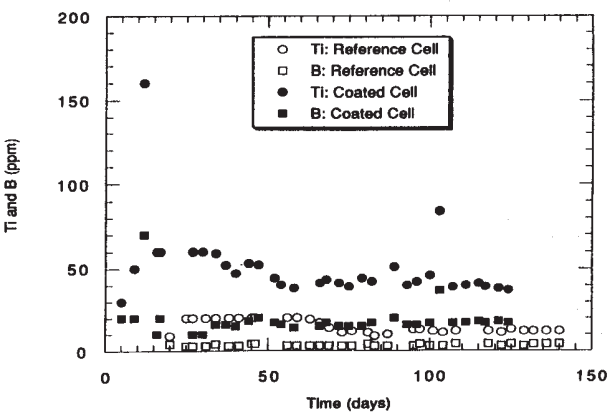

Figure 10: The content of Ti and B in aluminium from a 150 kA cell coated with alumina-bonded TiB_2 compared with reference cells.

This compares favourably with the published solubility product of TiB_2 of Finch [15] which is:

$$K = (\text{ppm Ti})\,(\text{ppm B})^2 = 1.21\cdot10^4 \text{ at } 960°C$$

Thus the dissolution of TiB_2 is governed by the equilibrium solubility product. This is further supported by the Ti / B ratio dissolved from this coating being 2.20 compared to the theoretical value of 2.22.

Assuming a current density of 0.8 A/cm^2 and 95 % current efficiency:

Produced Al = $0.8\cdot10^4\cdot60\cdot60\cdot24\cdot365\cdot0.95\cdot0.02698/3\cdot96485$ = $22.3\cdot10^3$ kg Al/year·m^2
Using the above data for the net dissolution of TiB_2 the average wear rate of the coating in this case will be 0.98 kg/m^2·year.

A coating of 3 kg/m^2 or more safely 4 kg/m^2 will hence last 3 years provided that the only mechanism is solution and not dislodgement of solid particles. On the other hand the wear rate will be reduced if the initial concentrations of Ti and B are increased. For instance, an increase of the initial boron concentration from 2.7 to 15 ppm will reduce the dissolution by 50 %.

Penetration of Sodium into Carbon with and without an Alumina-Bonded TiB_2 Coating

It has already been demonstrated in production cells that the alumina-bonded TiB_2 coating slows down the penetration of sodium into carbon with a strong decrease in the stress-causing sodium gradient during start-up [5]. In order to understand the mechanism of the barrier action, laboratory tests were conducted

using a modification of the inverse electrolysis test as described on p. 129-132 in ref. [6]. The modification was to sheath the samples with an alumina tube in order to get one dimensional penetration or migration (Fig. 11). Also the samples were not rotated.

Only the bottom part of the sample was coated with alumina-bonded TiB_2 and exposed to the electrolyte. The coating substrates were cores of electrocalcined anthracite with 30% graphite, baked to 1200°C with approximate dimensions 20 mm diameter and 60 mm length. The substrate samples were sealed into the alumina tube using a ceramic cement. Some of the substrate samples were coated (9 or 12 layers were applied) and the remainder were left uncoated as a reference. After application of each layer of coating the samples were allowed to dry naturally before the application of another layer. The increase in dry weight of the sample served as a measure of the coating loading and thickness.

The electrolytic bath used was alumina saturated with a cryolite ratio, CR, of 2.25, and 4 % CaF_2. Total bath weight was 380 g. An alumina crucible (external diameter 80 mm, internal diameter 70 mm and height 190 mm) contained the electrolyte while in a second alumina crucible acted as a guard. The crucibles were sheathed in an Inconel tube inside the furnace. Electrical connection from the alumina crucible, containing the bath, was made by using a graphite disc (27 cm^2) and alumina sheathed graphite rod joined to a tungsten rod. This disc served as the anode during electrolysis. The suspended cathode sample was held by a steel rod. The bottom of the specimen was immersed 2 mm below the melt surface. The electrolysis was performed at constant current using a nominal current density of 0.75 A/cm^2. The bath temperature was maintained at 1000°C. Current and voltage were recorded during electrolysis. During the period of electrolysis the height of the bath was maintained by the addition of cryolite and additives to maintain a constant composition and volume.

After 1 to 15 hours of electrolysis the samples were removed from the bath and cooled to room temperature. The samples were then disconnected from the steel support rod and cross-sectioned parallel to the longitudinal axis with a dry diamond saw.

For the coated specimens aluminium had penetrated into the pores but the coating still adhered strongly to the substrate. Contrasting the uncoated samples showed no adherence or wetting of the metal. The experiments with the uncoated samples showed unstable voltage probably because of the lack of sample rotation.

The penetration of sodium was measured by pressing moistened pH paper onto each half of the cathode sample and the distinct blue/purple colour change of the pH paper used as a measure of the sodium penetration [6].

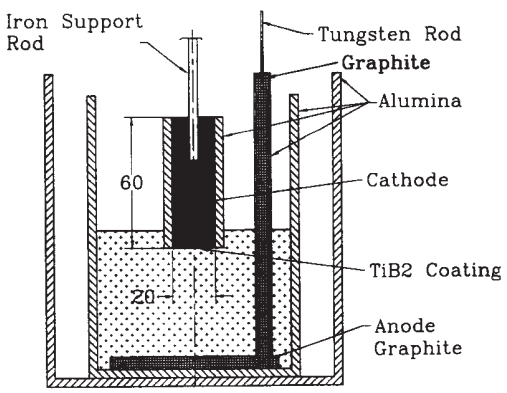

Figure 11: Cell arrangement for inverse electrolysis.

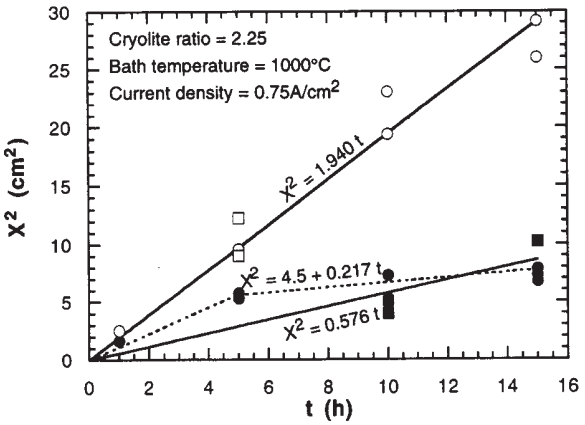

Figure 12: Square of sodium penetration, X^2, versus time, t, after reversed polarity experiments. ●: Anthracitic carbon with uncalcined TiB_2-coating. ■: Anthracitic carbon with calcined TiB_2-coating. o: Uncoated anthracitic carbon. □: Bulk alumina-bonded TiB_2.

The standard diffusional plot of the square of the height of the sodium penetration front *versus* electrolysis time [6] is shown in Fig. 12. The difference in the sodium penetration between the uncoated reference samples and the coated samples shows the retarding effect of the alumina-bonded TiB_2, thus acting as a sodium diffusion barrier.

The data of Fig. 12 can be extrapolated to a penetration length of 40 cm which is approximately the height of a cathode. It is found to be 34 days for an uncoated cathode and 116 days for a coated cathode if the straight line plots are used. If the TiB_2 coating is less effective at the start when not fully penetrated by aluminium, the broken line may be more appropriate. The time for full sodium penetration will then be 306 days. An accurate fit with industrial data which were respectively 55 and 290 days [5], and the laboratory results are not expected, but they agree within the right order of magnitude. Data for sodium penetration into bulk alumina-bonded TiB_2 are also included. This penetration is of the same order as uncoated material.

CONCLUDING DISCUSSION

During application the surface pores or defects of the carbon material are readily penetrated by the colloidal alumina-TiB_2 slurry (Fig. 5) because of its low viscosity and the fine TiB_2 grains (<15 μm). This penetration ensures a strong adherence of the coating to both to the cathode block and the ramming paste. The adherence withstands thermal cycling and has a bonding strength comparable or better than the surrounding carbon materials (Table III). No delamination was observed in spite of the difference in thermal expansion of the alumina-bonded TiB_2 material and the substrate carbon (Fig. 1). The mode of application as a slurry, the high porosity and high bonding strength of the coating are expected to be beneficial factors.

The alumina-bonded TiB_2 coating has a porosity of typically 30 %. The highly porous structure is visualized in Fig. 6. Calcination of the coating in the laboratory tests does not lead to sintering and densification but the bonding can best be described as a grain to grain contact with the small amount of calcined colloidal alumina acting as a glue. Despite this bonding the calcined material has an electrical conductivity of the same order as graphite. The high abrasion resistance (Table IV) is also an indirect indication of

strong bonding. The high abrasion resistance makes the coating especially valuable when utilized with the softer graphitic cathode materials. These materials are also most compatible with the alumina-bonded TiB_2 with respect to thermal expansion (Fig. 1). Wear due to abrasion is expected to be minimal but dissolution of TiB_2 by aluminium is expected to give a wear rate of approximately 0.3 mm/year. The alumina-bonded TiB_2 has the added advantage of not containing carbon so that aluminium carbide formation, which is the other contribution to cathode wear, cannot take place in the coating. The coating is susceptible to oxidation but an aluminium sheet placed on top of the coating before heat-up eliminates this reaction (Fig. 4). The coating is resistant to sodium when wetted by aluminium (Table I).

The wettability of the coating by liquid aluminium is a very important property. The wettability is demonstrated by the adherence of aluminium to the coating during electrolysis and the penetration of alumina into the pores (Fig. 7). The excellent wetting allows for more stable electrolysis conditions with possible energy and productivity gains. The wettability by liquid aluminium will also counteract the adhesion of frozen sludge / hard muck on the cathode surface which is a frequently occurring problem, especially in Søderberg operations.

The laboratory study of sodium uptake confirms industrial trials with the alumina-bonded TiB_2 coating which show that the sodium penetration into the carbon is slowed down [5]. Nevertheless sodium penetration is as fast into bulk alumina-bonded TiB_2 as in carbon. In carbon-bonded TiB_2 materials, sodium penetrates faster than in pure carbon materials [16].

The clue to these at first glance contradictory observations is the ability of the alumina-bonded TiB_2 to be wetted and penetrated by liquid aluminium. During electrolysis the pore structure of the coating will be filled with liquid aluminium. It is to be noted that the reaction

$$\text{Al (l)} + 3\ \text{NaF (in electrolyte)} = 3\ \text{Na (in C cathode)} + \text{AlF}_3\ \text{(in electrolyte)} \qquad (1)$$

needs three reactants to proceed, liquid aluminium, electrolyte and **carbon** which stabilize the formed sodium. The sodium codeposits in aluminium with a very small concentration without the presence of carbon. The stable aluminium layer in the pores (Fig. 7) and above the coating will prevent contact between the electrolyte and carbon so that the three reactants can no longer react directly. Sodium uptake is then limited by a slow diffusion of metallic sodium through the liquid aluminium. Contrasting, in industrial cells a layer of bath is present underneath the aluminium pool so that all three components are in close contact. The action of the alumina-bonded TiB_2 is hence not as a barrier by itself but the **ability to form a stable liquid aluminium barrier** at the surface of the carbon cathode thus increasing substantially the diffusion distance. In the bulk alumina-bonded TiB_2 or the bulk carbon-bonded TiB_2, the conditions for setting up a defined stable aluminium layer are not realized and the sodium penetration is not slowed down.

The studied coating usually had a thickness of up to 1 mm. Due to the solubility of TiB_2 in liquid aluminium, a greater thickness will be advantageous so that the TiB_2 coating will stay in place for the duration of cell operation. This is a requisite for drained-cell operation and so far there is reason to believe this goal will be achieved.

ACKNOWLEDGMENTS

Experimental assistance from Ms. W. Sørgård, Ms. A. Støre, Mr. K. Kvam and Mr. X. Liao at Institute of Inorganic Chemistry and Mr. Pierre-Alain Braillard and Mr. Enzo Zonca, at MOLTECH is gratefully appreciated. Thanks are also expressed to Heraeus Electrochemie for making the microscope pictures, Figs. 5 and 6.

REFERENCES

1. J. A. Sekhar and V. de Nora, "The Application of Refractory Borides to Protect Carbon-Containing Components of Aluminium Production Cells". PCT. WO 93/25731.

2. J. A. Sekhar, "Method of Reducing Erosion of Carbon-Containing Components of Aluminium Production Cells", U.S. Patent 5,534,119.

3. J. A. Sekhar, V. de Nora, J. Liu And J.-J. Duruz: "A Critical Analysis of Sodium Membranes to Prevent Carbon Cathode Damage in the Hall-Heroult Cell". Light Metals 1996, 271-276.

4. J. A. Sekhar, V. Bello, V. de Nora, J. Liu and J.-J. Duruz, "Cathode Coating for Improved Cell Performance", Light Metals 1995, 507-513

5. H. A. Øye, J. Thonstad, K. Dahlqvist, S. Handå and V. de Nora: "Reduction of Sodium Induced Stresses in Hall Heroult Cells", Aluminium 72 (1996) 000.

6. M. Sørlie and H. A. Øye: "Cathodes in Aluminium Electrolysis", Aluminium-Verlag, Düsseldorf, 1994, 408 pp.

7. Metals Reference Book. Ed. E. J. Smithells. 5th Ed., Butterworths, London (1978) p. 947.

8. H. Schreiner and H. A. Øye: "Sodium Expansion of Cathode Materials under Pressure", Light Metals 1995, 265-272.

9. W. Sørgård and H. A. Øye: "Adhesion between Ramming Pastes and Cathode Blocks in Aluminium Electrolysis Cells", CARBON '94, International Carbon Conference, Spanish Carbon Group and University of Granada, 818-819.

10. X. Liao and H.A. Øye. To be published.

11. P. A. Skjølsvik, J. Mittag and H. A. Øye: "Consumption of Cathode Materials Due to Al_4C_3 Formation", Aluminium 67 (1991) 905-909.

12. X. Liao and H. A. Øye: "Method for Determination of Abrasion Resistance of Carbon Cathode Materials at Room Temperature", Carbon 46 (1996) 649-661.

13. B. Berge, K. Grjotheim, C. Krohn, R. Næumann and K. Tørklep: "Recent Studies of Convection in Commercial Aluminium Reduction Cells", Metall Trans. 4 (1973) 1945-1952.

14. K. Dahlqvist, née Forsling: "Titanium Diboride Coated Cathodes in the Hall-Heroult Cell". M.Sc. Thesis Norwegian Institute of Technology, April 1995, 49 pp.

15. N. J. Finch, "The Mutual Solubilities of Titanium and Boron in Pure Aluminium", Metall Trans. 3 (1992) 2709-2711.

16. J. Xue and H. A. Øye, "Sodium and Bath Penetration into TiB_2-Carbon Cathodes during Laboratory Aluminium Electrolysis", Light Metals 1992, 773-778.